

# Electron-Ion Collider as a Discovery Tool for Invisible Dark Bosons

Hooman Davoudiasl<sup>1,\*</sup> and Hongkai Liu<sup>1,†</sup>

<sup>1</sup>High Energy Theory Group, Physics Department  
Brookhaven National Laboratory, Upton, NY 11973, USA

We illustrate how the future Electron-Ion Collider (EIC) can be used to discover dark bosons with masses in the  $\sim (10 \text{ MeV} - 10 \text{ GeV})$  regime, having a wide range of properties. We only require that the dark bosons have a non-negligible weak coupling to electrons and decay with  $\mathcal{O}(1)$  branching fraction into invisible final states. Our signal selection takes advantage of the excellent electron beam kinematic measurements and the capability to tag incoherent scattering, as envisioned at the EIC. This makes the EIC a powerful tool for uncovering potential dark sector forces, for a variety of possibilities.

## I. INTRODUCTION

While important fundamental questions remain open in particle physics and cosmology, there is currently no obvious hint where the answers may come from. Of these questions, the origin of neutrino masses and the nature of dark matter (DM) are two of the most pressing that we face today. Even though the evidence for these puzzles is not in doubt, the problem with either one – and some other fundamental mysteries – is that they can be resolved in a multitude of ways and over very wide ranges of parameters. This circumstance compels us to use every tool and all available methods to eliminate the allowed parameter space and, with a little help from luck, perhaps find a glimpse of the answers.

The Electron-Ion Collider (EIC), to be built over the coming years at the Brookhaven National Laboratory, aims to investigate the detailed structure of hadronic matter [1]. However, the capabilities of this new facility and its experiments can also lend themselves to searching for a variety of new phenomena that lie outside the Standard Model (SM) [2–20]. This possibility has gained significant attention in recent years and is worth further investigation. Given the parameters of the EIC, new physics at low mass scales with weak coupling to the SM would be a natural target for such experimental searches. These types of models have also been a focus of much attention over the last decade or so, and have been invoked in addressing various open questions [21]. In particular, such low scale physics may have its own “dark” or “hidden” sector that includes DM, as well as a number of other particles and forces that only indirectly interact with the SM, *i.e.* the “visible” world.

Motivated by the above considerations, in this work we will consider the detection of dark bosons, representing broad classes of models, at the EIC. We will only assume a very minimal set of requirements for the dark boson properties, mainly that: (i) it have a non-negligible weak coupling to electrons, and (ii) its decay have  $\mathcal{O}(1)$  branching fraction into invisible states. The first requirement stems from our focus on a production mechanism where the boson is emitted from the electron beam, in low momentum transfer coherent electromagnetic scattering from large atomic number  $Z$  ions, like

gold. This process would have a  $Z^2$  enhanced rate and can be quite important for producing GeV scale bosons emitted from the electron beam. The second requirement originates from our signal selection criteria that depend on the kinematics of beam electron upon dark boson emission. By focusing on invisible final states, we could avoid large SM backgrounds and have a clean signal. We note that the above conditions could be realized in a variety of models, including gauged  $B - L$  (with  $B$  and  $L$  baryon and lepton numbers, respectively) [22–24], gauged  $L_e - L_i$  models with  $i = \mu, \tau$  [25], dark  $Z$  models characterized by a dark vector mixing with the SM  $Z$  boson [26]; in these models neutrinos contribute significant branching fractions to the decay of the new vector boson. In general, one could also consider models where dark sector states, or neutrinos, constitute the main decay branching fraction of a dark boson, which could be a scalar or a vector.

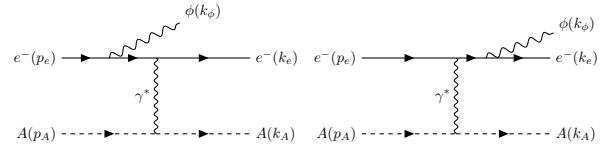


FIG. 1. Feynman diagrams of the  $\phi$  production via bremsstrahlung from the electron. We include both ISR (left panel) and FSR (right panel).

## II. BASIC MODELS

We will consider two cases: a scalar and a vector boson, both denoted by  $\phi$ . These will suffice to outline the broad classes of models that could be investigated at the EIC, using our proposed methodology. We consider the following generic interactions:

$$\begin{aligned}\mathcal{L}_S &= g_S^e \phi \bar{e}e + g_S^\chi \phi \bar{\chi}\chi, \\ \mathcal{L}_V &= g_V^e \phi_\mu \bar{e}\gamma^\mu e + g_V^\chi \phi_\mu \bar{\chi}\gamma^\mu \chi,\end{aligned}\quad (1)$$

where  $g_{S(V)}^e$  and  $g_{S(V)}^\chi$  are scalar (vector) couplings to electrons and  $\chi$ , respectively. The new boson  $\phi$  can be produced via the electron bremsstrahlung as shown in Fig. 1. We assume  $\chi$  is an invisible particle (SM neutrino or dark-sector particle) at the detector length scale and its mass  $m_\chi < m_\phi/2$ , so that  $\phi \rightarrow \bar{\chi}\chi$  is allowed on-shell. In principle,  $\chi$  could be

\* hooman@bnl.gov

† hliu6@bnl.gov

an SM particle or decay back to the SM particles, leading to a displaced vertex in the detector [13]. The combination of a displaced vertex and a depleted electron energy signal could potentially enhance the sensitivity. However, these scenarios require a more detailed analysis, which we leave for future work.

### III. ANALYSIS

The EIC can precisely measure the recoil electron and is capable of distinguishing between coherent scattering, where the nucleus remains intact, and incoherent scattering, where the nucleus breaks up, including through hard scattering and jet emission. In this work, we consider the coherent production of  $\phi$ , which benefits from a large  $Z^2$  enhancement for heavy nuclei such as gold. In the limit  $m_e \ll m_\phi \ll m_A \ll \sqrt{s}$ , the transferred momentum to the nucleus  $Q_A^2 \sim m_\phi^4 m_A^2 / s^2$ , where  $m_A$  denotes the ion mass and  $\sqrt{s}$  is the center of mass energy. The required  $Q_A^2$  increases rapidly with  $m_\phi$ . The ion-photon interaction vertex in the coherent regime is  $iV^\mu(Q_A^2, p_A, k_A) = ieZF(Q_A)(p_A + k_A)^\mu$ . The nuclear form factor  $F(Q_A)$  strongly suppresses contributions from  $\sqrt{Q_A^2}$  much larger than the inverse of the nucleus size,  $r_A^{-1} \sim (A^{1/3} \text{ fm})^{-1}$ , where  $A$  is the mass number of the nucleus. By assuming an electron beam energy 18 GeV and a 100 GeV per nucleon ion beam [1], we can estimate the maximum boson mass for coherent production  $(m_\phi)_{\text{max}} \sim 20 \text{ GeV} (197/A)^{1/6}$ . The production cross sections drop sharply with increasing  $m_\phi$  as shown by the black curves in Fig. 2. The amplitude squared and phase space integration are discussed in detail in [13, 14]. To account for the nuclear charge distribution at low momentum transfer, we use the Helm form factor [27]

$$F(Q_A) = \frac{3j_1(Q_A R_1)}{Q_A R_1} \exp\left[-\frac{(Q_A \rho)^2}{2}\right], \quad (2)$$

where  $j_1$  is the first spherical Bessel function of the first kind,  $\rho = 0.9 \text{ fm}$  and  $R_1 \simeq 1.1 \text{ fm} A^{1/3}$ . We find similar kinematics for scalar and vector dark boson  $\phi$ . Therefore, in the following, we present only the results for the vector boson. Our final projections for the coupling  $g_\phi^e$  can be obtained for the scalar case by simple scaling of the cross section  $\sigma_\phi$ , via the relation  $\sqrt{\sigma_\phi} \propto g_\phi^e$ .

The new boson  $\phi$  with a mass of  $\mathcal{O}(\text{GeV})$  carries away most of the electron beam energy, leaving a soft electron in the final state. Therefore, the transferred momentum on the electron side ( $Q_e^2$ ) is significantly larger than that on the ion side ( $Q_A^2$ ), as illustrated in Fig. 3. This behavior differs from the SM coherent scattering, where both the electron and ion experience low and comparable momentum transfer. The distributions of transverse momentum  $p_T^e$  and pseudorapidity  $\eta_e$  of the recoil electrons are shown in Fig. 4, for three representative  $\phi$  masses. As the virtual photon exchanged between the ion and electron becomes harder for heavier  $\phi$ , the recoil electron tends to shift towards the central region and can even move in the forward direction in the production of  $\mathcal{O}(\text{GeV})$  scale  $\phi$ .

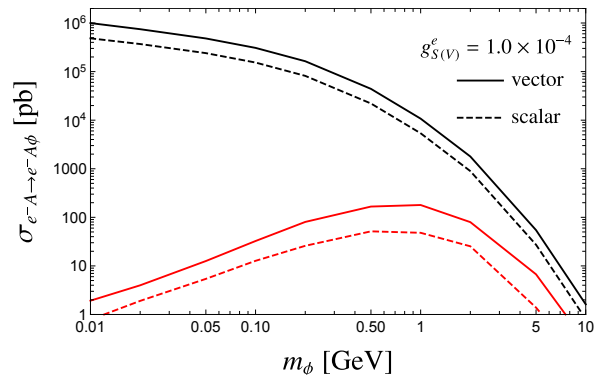


FIG. 2. The production cross sections of  $\phi$  via the electron bremsstrahlung. The solid (dashed) black line shows the production cross section of vector (scalar) new boson. The red lines show the corresponding production cross sections after applying the cuts in Eq. (3).

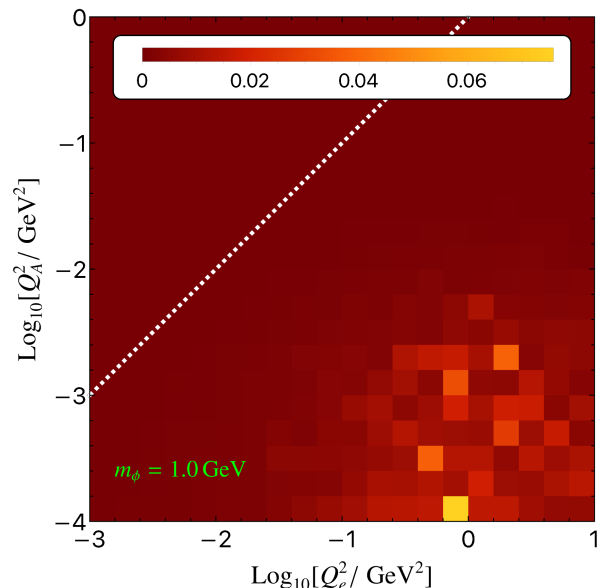


FIG. 3. The correlation between  $Q_e^2$  and  $Q_A^2$  in the presence of  $\phi$  with a mass of 1.0 GeV. The dashed white line represents the SM background expectation.

One of the main backgrounds to the above  $\phi$  production process is the SM bremsstrahlung  $e^- A \rightarrow e^- A \gamma$ , where the photon is missed. In contrast to the massive vector dark boson production in the signal, the SM bremsstrahlung background typically features soft and collinear photons. The electron distributions are depicted by the black lines in Fig. 4. Therefore, we apply the following cuts to select events with central electrons of large transverse momentum to suppress the SM bremsstrahlung background

$$|\eta_e| < 3.5, p_T^e > 1.2 \text{ GeV}, E_e < 10 \text{ GeV}, Q_e^2 > 4 \text{ GeV}^2, \quad (3)$$

where  $E_e$  is the energy of the recoil electron. The signal cross sections after applying the cuts are given by the red lines in

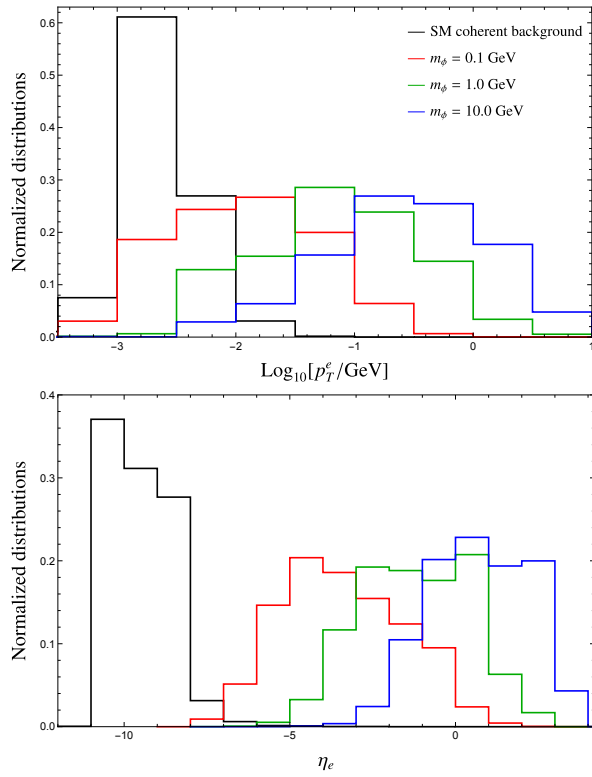


FIG. 4. The recoil electron distributions of transverse momentum (upper panel) and pseudorapidity (lower panel).

Fig. 2, which as expected from the preceding discussion are significantly more suppressed in the low  $m_\phi$  regime. Since we select recoil electrons with energy less than 10 GeV, the photon energy in the SM bremsstrahlung is mostly larger than 5 GeV. We assume that the inefficiency for 5 GeV central photons is  $10^{-6} \leq \epsilon \leq 10^{-5}$  [28, 29]. In our analysis, the chance of missing such energetic photons is conservatively taken to be 100%, when  $|\eta_\gamma| > 3.5$ . The effective SM bremsstrahlung cross sections after applying the cuts are around  $7.0 \times \epsilon/10^{-5}$  pb and 0.1 pb for  $|\eta_\gamma| < 3.5$  and  $|\eta_\gamma| > 3.5$ , respectively.

Another main background is the SM deep inelastic scattering (DIS)  $e^- A \rightarrow e^- X j$ , where  $X$  denotes nuclear hadronic debris and the jet  $j$  is missed. Since the EIC detector operational capabilities are not established and an envisioned second detector has not been defined yet, we only focus on the gross features of the signal, such as the expected total hadronic energy in the central detector. For this purpose, we show the results at parton level and use the Mathematica package ManeParse [30] to implement the parton distribution functions. The jet  $j$  is defined as the final-state quark in the DIS process. The background from the SM DIS process  $eA \rightarrow eXj$  after the cuts is  $4.0 \times 10^4$  pb. Below, we argue that this large background can be sufficiently reduced.

Our calculations show that the jet produced in the DIS process is central ( $|\eta_j| < 3.5$ ), with a minimum transverse

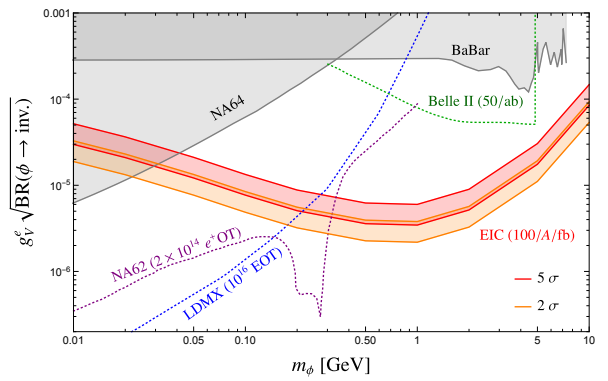


FIG. 5. The EIC projections for the electron coupling  $g_V^e$  of an invisibly decaying dark vector  $\phi$  with fraction  $\text{BR}(\phi \rightarrow \text{inv.})$ . The  $5\sigma$  and  $2\sigma$  bands are shown in red and orange, respectively. An integrated luminosity of  $100/A \text{ fb}^{-1}$  has been assumed for  $Z = 79$ , corresponding to gold ions. The current constraints are shaded in gray [34, 35]. The Belle-II [36, 37], LDMX [38, 39], and NA62 [40] projections are overlaid for comparison.

momentum of 1.2 GeV and a minimum energy of 8 GeV<sup>1</sup>. Therefore, similar to the SM bremsstrahlung, we expect significant activity in the central detector due to the jet emission. Additionally, the DIS background can be reduced significantly by the veto of incoherent scattering at the Zero Degree Calorimeter [1] in the far-forward direction with an efficiency  $\gtrsim 95\%$  [32, 33]. Hence, we assume that the DIS background is suppressed by an inefficiency  $10^{-6} \leq \epsilon \leq 10^{-5}$  for missing such an energetic and central jet, similar to the coherent background discussed earlier. The effective DIS background is estimated as  $\lesssim 0.02 \times \epsilon/10^{-5}$  pb. We note that the DIS background can be enhanced by a factor of  $Z$  to account for the corresponding  $ep$  luminosity. Therefore, the DIS background is smaller but comparable to that of the bremsstrahlung process. The cross section of the SM irreducible background  $e^- A \rightarrow e^- A \nu \bar{\nu}$  mediated by the massive weak gauge bosons is found to be negligible compared to the previous two background processes.

The signal cross sections after the cuts are shown by the red curve in Fig. 2. To estimate the reach of the EIC, we require  $S/\sqrt{B} = 2$  and  $5$  with  $100/A \text{ fb}^{-1}$  integrated  $eA$  luminosity (assuming ultimate design luminosity). Here,  $S$  and  $B$  are the numbers of signal and background events, respectively. The  $2$  ( $5$ ) $\sigma$  projection for the reach of the EIC is shown by the red (orange) band in Fig. 5. The width of the band reflects the uncertainty in the detector inefficiency  $\epsilon$ . The most stringent bounds of the invisible decay dark vector boson are from the mono-photon search at BaBar [34] and the missing momentum search at NA64 [35].

As can be seen from Fig. 5, the EIC has the potential to probe a wide range of open parameter space for dark bosons, as long as they have a non-negligible branching fraction into modes that are invisible on detector transit time scales. In

<sup>1</sup> We have validated our calculations against MadGraph5\_aMC@NLO [31].

particular, for such bosons over the mass range  $\sim (0.3 - 10)$  GeV, the projected EIC constraints on the associated models are better than those of current or envisioned experiments in the future.

#### IV. SUMMARY

In this work, we have considered the potential for the EIC to uncover the signals of dark bosons that couple weakly to electrons and decay with significant invisible branching fraction. These bosons, vectors or scalars, can originate from a broad class of models. The invisible final states can be neutrinos, or they may be light states from a dark sector that escape the detector due to their sufficiently long lifetimes.

We examine a search strategy that leverages the excellent electron detection capabilities of the future EIC experiments, where emission of the invisible boson leads to considerable depletion of the electron beam energy and imparts a significant transverse momentum to it. The production process we consider is based on coherent scattering of the electron from

a high  $Z$  ion, like gold, and leads to a large cross section. The intact ion in this process also provides another handle on signal identification. The main background, from the analogue process with the emission of a hard GeV scale photon (coherent) or jet (DIS), can be suppressed assuming realistic detection efficiencies. The projected parameter space that can be probed for these models is broad and extends well beyond those accessed in the future, by current or proposed experiments. We conclude that the EIC can play a significant role in the experimental investigations of dark sector forces in a wide variety of interesting models.

The digital data associated with this work can be found as ancillary files with the arXiv submission [41].

#### ACKNOWLEDGMENTS

We thank A. Jentsch for helpful discussions regarding experimental issues. This work is supported by the US Department of Energy under Grant Contract DE-SC0012704.

- 
- [1] R. Abdul Khalek *et al.*, Science Requirements and Detector Concepts for the Electron-Ion Collider: EIC Yellow Report, *Nucl. Phys. A* **1026**, 122447 (2022), [arXiv:2103.05419 \[physics.ins-det\]](#).
  - [2] M. Gonderinger and M. J. Ramsey-Musolf, Electron-to-Tau Lepton Flavor Violation at the Electron-Ion Collider, *JHEP* **11**, 045, [Erratum: *JHEP* 05, 047 (2012)], [arXiv:1006.5063 \[hep-ph\]](#).
  - [3] R. Boughezal, F. Petriello, and D. Wiegand, Removing flat directions in standard model EFT fits: How polarized electron-ion collider data can complement the LHC, *Phys. Rev. D* **101**, 116002 (2020), [arXiv:2004.00748 \[hep-ph\]](#).
  - [4] Y. Liu and B. Yan, Searching for the axion-like particle at the EIC\*, *Chin. Phys. C* **47**, 043113 (2023), [arXiv:2112.02477 \[hep-ph\]](#).
  - [5] V. Cirigliano, K. Fuyuto, C. Lee, E. Mereghetti, and B. Yan, Charged Lepton Flavor Violation at the EIC, *JHEP* **03**, 256, [arXiv:2102.06176 \[hep-ph\]](#).
  - [6] H. Davoudiasl, R. Marcarelli, and E. T. Neil, Lepton-flavor-violating ALPs at the Electron-Ion Collider: a golden opportunity, *JHEP* **02**, 071, [arXiv:2112.04513 \[hep-ph\]](#).
  - [7] B. Yan, Z. Yu, and C. P. Yuan, The anomalous  $Zbb^-$  couplings at the HERA and EIC, *Phys. Lett. B* **822**, 136697 (2021), [arXiv:2107.02134 \[hep-ph\]](#).
  - [8] H. T. Li, B. Yan, and C. P. Yuan, Jet charge: A new tool to probe the anomalous  $Zbb^-$  couplings at the EIC, *Phys. Lett. B* **833**, 137300 (2022), [arXiv:2112.07747 \[hep-ph\]](#).
  - [9] B. Batell, T. Ghosh, T. Han, and K. Xie, Heavy neutral leptons at the Electron-Ion Collider, *JHEP* **03**, 020, [arXiv:2210.09287 \[hep-ph\]](#).
  - [10] J. L. Zhang *et al.*, Search for  $e \rightarrow \tau$  charged lepton flavor violation at the EIC with the ECCE detector, *Nucl. Instrum. Meth. A* **1053**, 168276 (2023), [arXiv:2207.10261 \[hep-ph\]](#).
  - [11] B. Yan, Probing the dark photon via polarized DIS scattering at the HERA and EIC, *Phys. Lett. B* **833**, 137384 (2022), [arXiv:2203.01510 \[hep-ph\]](#).
  - [12] R. Boughezal, A. Emmert, T. Kutz, S. Mantry, M. Nycz, F. Petriello, K. Şimşek, D. Wiegand, and X. Zheng, Neutral-current electroweak physics and SMEFT studies at the EIC, *Phys. Rev. D* **106**, 016006 (2022), [arXiv:2204.07557 \[hep-ph\]](#).
  - [13] H. Davoudiasl, R. Marcarelli, and E. T. Neil, Displaced signals of hidden vectors at the Electron-Ion Collider, *Phys. Rev. D* **108**, 075017 (2023), [arXiv:2307.00102 \[hep-ph\]](#).
  - [14] R. Balkin, O. Hen, W. Li, H. Liu, T. Ma, Y. Soreq, and M. Williams, Probing axion-like particles at the Electron-Ion Collider, *JHEP* **02**, 123, [arXiv:2310.08827 \[hep-ph\]](#).
  - [15] H. Davoudiasl, R. Marcarelli, and E. T. Neil, Flavor-violating ALPs, electron g-2, and the Electron-Ion Collider, *Phys. Rev. D* **109**, 115013 (2024), [arXiv:2402.17821 \[hep-ph\]](#).
  - [16] H.-L. Wang, X.-K. Wen, H. Xing, and B. Yan, Probing the four-fermion operators via the transverse double spin asymmetry at the Electron-Ion Collider, *Phys. Rev. D* **109**, 095025 (2024), [arXiv:2401.08419 \[hep-ph\]](#).
  - [17] X.-K. Wen, B. Yan, Z. Yu, and C. P. Yuan, Dihadron azimuthal asymmetry and light-quark dipole moments at the Electron-Ion Collider, (2024), [arXiv:2408.07255 \[hep-ph\]](#).
  - [18] Q. Gao, D. Lin, H. Liu, and T. Ma, Dark photons and axion-like particles at the Electron-Ion Collider in China, (2024), [arXiv:2412.06301 \[hep-ph\]](#).
  - [19] Y. Du, Parity Violation on Longitudinal Single-Spin Asymmetries at the EicC, (2024), [arXiv:2412.20469 \[hep-ph\]](#).
  - [20] Y. Deng, X.-H. Jiang, T. Liu, and B. Yan, Testing Lepton Flavor Universality at the Electron-Ion Collider, (2025), [arXiv:2503.02605 \[hep-ph\]](#).
  - [21] J. Alexander *et al.*, Dark Sectors 2016 Workshop: Community Report (2016) [arXiv:1608.08632 \[hep-ph\]](#).
  - [22] R. N. Mohapatra and J. C. Pati, Left-Right Gauge Symmetry and an Isoconjugate Model of CP Violation, *Phys. Rev. D* **11**, 566 (1975).
  - [23] R. N. Mohapatra and J. C. Pati, A Natural Left-Right Symmetry, *Phys. Rev. D* **11**, 2558 (1975).
  - [24] G. Senjanovic and R. N. Mohapatra, Exact Left-Right Symme-

- try and Spontaneous Violation of Parity, *Phys. Rev. D* **12**, 1502 (1975).
- [25] X. G. He, G. C. Joshi, H. Lew, and R. R. Volkas, NEW Z-prime PHENOMENOLOGY, *Phys. Rev. D* **43**, 22 (1991).
- [26] H. Davoudiasl, H.-S. Lee, and W. J. Marciano, 'Dark' Z implications for Parity Violation, Rare Meson Decays, and Higgs Physics, *Phys. Rev. D* **85**, 115019 (2012), [arXiv:1203.2947 \[hep-ph\]](#).
- [27] R. H. Helm, Inelastic and Elastic Scattering of 187-Mev Electrons from Selected Even-Even Nuclei, *Phys. Rev.* **104**, 1466 (1956).
- [28] Y. Maeda *et al.*, An aerogel Cherenkov detector for multi-GeV photon detection with low sensitivity to neutrons, *PTEP* **2015**, 063H01 (2015), [arXiv:1412.6880 \[physics.ins-det\]](#).
- [29] J. Fry *et al.* (KOTO), Proposal of the KOTO II experiment, (2025), [arXiv:2501.14827 \[hep-ex\]](#).
- [30] D. B. Clark, E. Godat, and F. I. Olness, ManeParse : A Mathematica reader for Parton Distribution Functions, *Comput. Phys. Commun.* **216**, 126 (2017), [arXiv:1605.08012 \[hep-ph\]](#).
- [31] J. Alwall, M. Herquet, F. Maltoni, O. Mattelaer, and T. Stelzer, MadGraph 5 : Going Beyond, *JHEP* **06**, 128, [arXiv:1106.0522 \[hep-ph\]](#).
- [32] W. Chang, E.-C. Aschenauer, M. D. Baker, A. Jentsch, J.-H. Lee, Z. Tu, Z. Yin, and L. Zheng, Investigation of the background in coherent  $J/\psi$  production at the EIC, *Phys. Rev. D* **104**, 114030 (2021), [arXiv:2108.01694 \[nucl-ex\]](#).
- [33] E.-C. Aschenauer, A. Bazilevsky, A. Jentsch, J. Kim, A. Kiselev, B. Page, Z. Tu, T. Ullrich, and C.-P. Wong, Tagging efficiency study of incoherent diffractive vector meson production at the second interaction region at the Electron-Ion Collider, *Phys. Rev. D* **111**, 072013 (2025), [arXiv:2501.12410 \[physics.ins-det\]](#).
- [34] J. P. Lees *et al.* (BaBar), Search for Invisible Decays of a Dark Photon Produced in  $e^+e^-$  Collisions at BaBar, *Phys. Rev. Lett.* **119**, 131804 (2017), [arXiv:1702.03327 \[hep-ex\]](#).
- [35] Y. M. Andreev *et al.* (NA64), Search for Light Dark Matter with NA64 at CERN, *Phys. Rev. Lett.* **131**, 161801 (2023), [arXiv:2307.02404 \[hep-ex\]](#).
- [36] R. Essig, J. Mardon, M. Papucci, T. Volansky, and Y.-M. Zhong, Constraining Light Dark Matter with Low-Energy  $e^+e^-$  Colliders, *JHEP* **11**, 167, [arXiv:1309.5084 \[hep-ph\]](#).
- [37] W. Altmannshofer *et al.* (Belle-II), The Belle II Physics Book, *PTEP* **2019**, 123C01 (2019), [Erratum: PTEP 2020, 029201 (2020)], [arXiv:1808.10567 \[hep-ex\]](#).
- [38] E. Izaguirre, G. Krnjaic, P. Schuster, and N. Toro, Testing GeV-Scale Dark Matter with Fixed-Target Missing Momentum Experiments, *Phys. Rev. D* **91**, 094026 (2015), [arXiv:1411.1404 \[hep-ph\]](#).
- [39] E. Izaguirre, G. Krnjaic, P. Schuster, and N. Toro, Analyzing the Discovery Potential for Light Dark Matter, *Phys. Rev. Lett.* **115**, 251301 (2015), [arXiv:1505.00011 \[hep-ph\]](#).
- [40] F. Arias-Aragón, L. Darmé, R. Gargiulo, G. G. di Cortona, V. Kozhuharov, E. Nardi, M. Raggi, T. Spadaro, and P. Valente, NA62e+: dark sector searches with high intensity positron beams in ECN3, (2025), [arXiv:2502.10346 \[hep-ph\]](#).
- [41] The digital daate can be found at: <https://arxiv.org/abs/2505.08871>.